Reduction of lattice thermal conductivity in one-dimensional quantum-dot superlattices due to phonon filtering

D. L. Nika* and E. P. Pokatilov
Laboratory PMSMM, Department of Theoretical Physics, Moldova State University, Chisinau, MD-2009, Republic of Moldova

A. A. Balandin
Nano-Device Laboratory, Department of Electrical Engineering, University of California–Riverside, Riverside, CA 92521, USA

V. M. Fomin, A. Rastelli, and O. G. Schmidt
Institute for Integrative Nanosciences, IFW-Dresden, Dresden D-01069, Germany
(Received 23 January 2011; revised manuscript received 19 May 2011; published 10 October 2011)

One dimensional quantum-dot superlattices (1D-QDSLs) consisting of acoustically mismatched materials are demonstrated theoretically to possess sub-1 W m^{-1} K^{-1} thermal conductivity in the 50–400 K range of temperatures. We consider coherent Si/Ge 1D-QDSLs, as well as model Si/plastic, Si/SiO_2 and Si/SiC 1D-QDSLs. The phonon energy spectra and group velocities are obtained in the framework of the face-centered cubic cell model of lattice dynamics. On this basis, lattice thermal conductivity is calculated. A strong reduction of lattice thermal conductivity in 1D-QDSL structures in comparison with homogeneous rectangular Si nanowires is explained by the exclusion of phonon modes folded in superlattice segments from the heat flow and by the decelerating action of Ge, SiO_2, or plastic materials. Thus, the 1D-QDSL structures act as effective phonon filters, eliminating a significant number of phonon modes from thermal transport. The obtained results imply a perspective of quantum-dot superlattices as thermoelectric materials and thermal insulators.

DOI: 10.1103/PhysRevB.84.165415 PACS number(s): 63.22.Kn, 65.80.−g, 63.22.Gh, 63.20.D−

I. INTRODUCTION

A reduction in the size and a corresponding increase in the density of elements on a chip make the task of improving thermal conductivity an important problem in modern electronics.[1–3] Insufficient heat removal from devices implies they could overheat, which degrades their performance and limits the operating frequency. However, decrease of thermal conductivity may improve the quality of thermoelectrics. The efficiency of thermoelectric devices is determined by the dimensionless figure of merit $ZT = S^2\sigma T/(\kappa_{ph} + \kappa_{el})$, where S is the Seebeck coefficient, σ is the electrical conductivity, T is the absolute temperature, and κ_{ph} and κ_{el} are the lattice (phonon) and electronic thermal conductivity, respectively. One possible way to increase the figure of merit consists of achieving low values of thermal conductivity while maintaining good electronic transport characteristics (electrical conductivity and Seebeck coefficient) in phonon-blocking and electron-transmitting nanostructures.[4]

In technologically important semiconductor devices, acoustic phonons play a dominant role in lattice thermal conductivity. The thermal conductivity of semiconductor nanoscale structures is much lower than the corresponding bulk value[3,5–7] due to the increase in phonon scattering at the boundaries of a nanostructure and the modification of the phonon energy spectrum, leading to a decrease in phonon group velocity.[3,5–9] It has been demonstrated theoretically that lattice thermal conductivity in Si free-standing films[5] and Si nanowires[6,7] is two orders of magnitude lower than the corresponding bulk value. Measurements of thermal conductivity in single free-standing Si nanowires with diameters of 22–115 nm confirmed the theoretical prediction and showed a decrease in thermal conductivity by two orders of magnitude[10] in comparison with that in bulk silicon.

Thermal conductivity of different nanostructures (quantum layers,[9,11,12] nanowires with different cross section shapes and sizes,[6,7,13–17] and quantum-dot superlattices[18–21]) has been a subject of wide theoretical and experimental interest. For calculation of thermal conductivity, researchers often use the phonon energy spectra obtained in the framework of the continuum approach, which gives correct dispersion relations in the long-wave limit. Zou *et al.*[22] theoretically investigated thermal conductivity in planar AlN/GaN/AlN heterostructures by taking into account the spatial confinement of shear phonon modes.

In Ref. 11, in the framework of the continuum approach, lattice thermal conductivity of dilatational and shear phonon modes was calculated in planar three-layer Si/Ge/Si heterostructures. The authors found that thermal conductivity of a conducting Ge channel could be adjusted by suitable selection of barrier layer thickness and the boundary scattering parameter. In Ref. 14, thermal conductivity of rectangular nanowires made of CdTe was studied. It was found that the phonon confinement led to a substantial reduction of lattice thermal conductivity at relatively low temperatures. However, the continuum approach is inadequate to describe the short-length, high-energy phonon modes that are significant for heat transfer. Recently, it has been demonstrated[23] that the continuum approach significantly overestimates thermal conductivity for medium and high temperatures ($T > 100$ K) in comparison with the face-centered cubic cell (FCC) model of lattice dynamics due to a steep slope of the dispersion curves for high-frequency phonon modes. Models of lattice dynamics,[13,23–28] which are valid for all values of the phonon wave vector, allow for an accurate description of the thermal properties of nanostructures that is in a good agreement with experimental data on thermal conductivity.

In the present paper, using the FCC model of lattice dynamics, we show that we can achieve a drop in lattice thermal conductivity in a nanowire consisting of segments made of different materials—one-dimensional quantum-dot superlattice (1D-QDSL)—due to a strong decrease in phonon group velocities. The great advantage of 1D-QDSLs in comparison with planar superlattices,[29–31] is that elastic stresses relax more easily in 1D-QDSLs than in superlattices from quantum layers due to the small structure dimensions in the plane perpendicular to the nanowire axis. The latter helps ensure defect-free interfaces. Femtosecond ultrasonic transport of coherent acoustic phonons with energies of the order of and less than the forbidden band of three-dimensional Si/Ge quantum-dot superlattices[32] revealed that the three-dimensional ordering and uniformity of the quantum dots strongly influence the acoustic resonance observed at the phononic band gap. The efficiency of quantum-dot superlattices in thermoelectricity was discussed in the literature,[33] with focus on the electronic properties of 1D-QDSLs. Recently, the role of electron minibands in the enhancement of thermoelectric efficiency in GaAs/InAs 1D-QDSLs has been theoretically analyzed.[34] In the present paper, we focus on an investigation of the phonon properties and lattice thermal conductivity of 1D-QDSLs.

The rest of the paper is organized as follows. In Sec. II, we describe the theoretical model for acoustic phonons and the method of calculation of thermal conductivity in the nanowires and 1D-QDSLs. Results and discussions are presented in Sec. III. We give our conclusions in Sec. IV.

II. THEORETICAL MODEL

We investigate acoustic and heat-conducting properties of rectangular Si and Ge nanowires, as well as 1D-QDSLs in the framework of the FCC model of lattice dynamics.[18,23,28] The crystal lattice of silicon consists of two FCC sublattices, which are shifted along the main diagonal of a unit cell by 1/4 of its length. In the FCC model, two shifted FCC sublattices are considered a common FCC lattice with double mass at each lattice node. This simplification neglects the optical phonon modes. However it is adequate since thermal conductivity in semiconductors is mainly determined by the acoustic phonons. Our model is based on three force constants, which are expressed through independent elastic constants of a material. This allows us to simulate the acoustic properties of heterostructures consisting of layers with different acoustic properties and various dimensions.[23,28] The schemes of a rectangular nanowire and a 1D-QDSL in vacuum are shown in Fig. 1. The external surfaces of the considered nanostructures

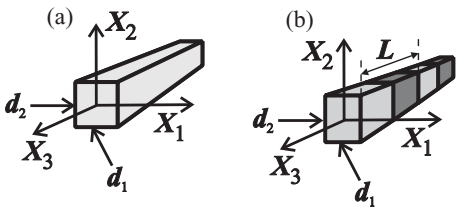

FIG. 1. Schematic view of the nanostructures: (a) a rectangular nanowire and (b) a 1D-QDSL.

are assumed to be free.[6,8,9] The X_1 and X_2 axes of the Cartesian coordinate system are located in the plane of the cross section of the nanowire and are parallel to its sides, while the X_3 axis is directed along the axis of the nanowire. We suppose that the length of the nanowire along axis X_3 is infinite. The origin of coordinates is at the center of the cross section of the nanowire. The lengths of sides of the nanowire are denoted as d_1 and d_2, respectively, while the period of 1D-QDSL is denoted as L.

In the FCC model, all lattice nodes in bulk materials are translationally equivalent. The displacement of a lattice atom in the node labeled with the number $\vec{n}$ can be written as

$$\vec{u}(\vec{n}) = \vec{w}(\vec{q})e^{i(\vec{q}\vec{n}-\omega t)}. \tag{1}$$

Because of the equivalence of nodes, the amplitude of their displacements does not depend on the node number: $\vec{n} = \vec{a}_1 n_1 + \vec{a}_2 n_2 + \vec{a}_3 n_3$, where $\vec{a}_1 = \frac{a}{2}(0,1,1)$, $\vec{a}_2 = \frac{a}{2}(1,1,0)$, and $\vec{a}_3 = \frac{a}{2}(1,0,1)$ are basis vectors of the FCC; n_1, n_2, and n_3 are integers; and a is the lattice constant, with $a(\mathrm{Si}) = 0.549$ nm and $a(\mathrm{Ge}) = 0.565$ nm.

The node displacement in a bulk crystal is described by the vectorial equation of motion with three components

$$m\ddot{u}_i(\vec{n}) = F_i(\vec{n}), \quad i = 1,2,3, \tag{2}$$

where $F_i(\vec{n})$ is a component of the force acting on node $\vec{n}$ from the other nodes of the lattice and m is the node mass (double atomic mass in the framework of the FCC model). In the harmonic approximation,

$$F_i(\vec{n}) = -\frac{\partial V}{\partial u_i(\vec{n})} = -\sum_{\vec{n}',j} \Phi_{ij}(\vec{n},\vec{n}')u_j(\vec{n}'), \tag{3}$$

where $\Phi_{ij}(\vec{n},\vec{n}')$ is the three-dimensional matrix of the force constants and V is the potential energy of the lattice.

Taking into account Eq. (1), we obtain

$$m\omega^2 w_i(\vec{q}) = \sum_{j=1,2,3} D_{ij}(\vec{q})w_j(\vec{q}), \tag{4}$$

where $D_{ij}(\vec{q}) = \sum_{\vec{h}} \Phi_{ij}(0,\vec{h})e^{i\vec{q}\vec{h}}$ is the dynamic matrix and $\vec{h} = \vec{n}' - \vec{n}$.

We take into account the interaction of the node with the nearest and second-nearest nodes. The interaction with the 12 nearest nodes is centrally symmetric, and it is described by one constant, α_1.[35] The matrix of the force constants in this case is $\Phi_{il}(\vec{n}',\vec{n}) = -\alpha_1(\vec{n}',\vec{n})h_i^1 h_l^1/(h^1)^2$, where $\vec{h}^1$ indicates the positions of the nearest nodes of node $\vec{n} = 0$ and h_i^1 is the projection of vector $\vec{h}^1$ on the corresponding coordinate axis X_i. The interaction with the second-nearest nodes is not centrally symmetric, and it is described by two constants, α and β.[36,37] The vector $\vec{h}^2$ describes the position of the six second-nearest nodes of node $\vec{n} = 0$:

$$\begin{aligned}
&\Phi_{ij}(0,\vec{h}^2 = a(\pm 1,0,0)) = -\delta_{ij}\gamma_{ii}, \quad \gamma_{11} = \alpha; \gamma_{22} = \gamma_{33} = \beta \\
&\Phi_{ij}(0,\vec{h}^2 = a(0,\pm 1,0)) = -\delta_{ij}\gamma_{ii}, \quad \gamma_{11} = \gamma_{33} = \beta; \gamma_{22} = \alpha \\
&\Phi_{ij}(0,\vec{h}^2 = a(0,0,\pm 1)) = -\delta_{ij}\gamma_{ii}, \quad \gamma_{11} = \gamma_{22} = \beta; \gamma_{33} = \alpha.
\end{aligned} \tag{5}$$

For every node with vector $\vec{h}$ there exists a node with vector $-\vec{h}$; therefore, the dynamic matrix is real. Comparing the phonon dispersions $\omega(q)$ for three phonon branches (one longitudinal and two transversal) obtained from Eq. (4) in the long-wave limit $q \to 0$ with those derived within a continuum approach,[9] we established the following relations between the constants α_1, α, and β and the elastic moduli of a cubic crystal c_{11}, c_{12}, and c_{44}: $\alpha_1 = a(c_{12}+c_{44})/2$, $\alpha = a(c_{11} - c_{12} - c_{44})/4$, and $\beta = a(c_{44} - c_{12})/8$. Using these relations, we calculate the phonon energy spectra in nanostructures.

We select the X_3 axis of the nanowire along the (0 0 1) direction of the cubic crystal and assume that a lattice node exists at the origin of coordinates. Translational symmetry in the considered nanostructures is preserved only along nanostructure axis X_3. Therefore, the equivalent lattice nodes in the nanostructure are located on lines parallel to axis X_3, which passes through the center of the nanowire. Displacements of equivalent nodes have one amplitude,

$$\vec{u}(\vec{n}) = \vec{w}(x_1,x_2,q)e^{iqh_3^k}, \tag{6}$$

where x_1 and x_2 are coordinates of the points of intersection of those lines with the (X_1,X_2)-plane and $k = 1,2$ is the number of the coordination sphere. The number of nonequivalent nodes in the nanowire is equal to the number of the intersection points. The nodes are partly located directly on the plane and partly shifted by $a/2$ along X_3. The number of equations of motion is triple the number of the intersection points: $3N$.

The equations of motion for the nanowire have the form

$$m\omega^2 w_i(x_1,x_2;q) = \sum_{j=1,2,3;x_1',x_2'} D_{ij}(x_1,x_2;x_1',x_2';q) \times w_j(x_1',x_2';q), \tag{7}$$

where

$$D_{ij}(x_1,x_2;x_1',x_2';q) = \sum_{h_3^k} \Phi_{ij}^k(\vec{n},\vec{n}+\vec{h}^k)e^{iqh_3^k}. \tag{8}$$

The summation in Eq. (8) is performed over all nearest and second-nearest nodes, which are equivalent to node (x_1,x_2), i.e., are located on the same line. The vector $\vec{n}$ has the form $\vec{n} = (x_1,x_2,0)$ when the node is located on the (X_1,X_2)-plane and $\vec{n} = (x_1,x_2,a/2)$ otherwise. Invariance of the set in the form of Eq. (7) with respect to the reflection in the planes of symmetry leads to the following four possible types of solutions:[17]

Dilatational (D): $w_1^{AS}(x_1,x_2); w_2^{SA}(x_1,x_2); w_3^{SS}(x_1,x_2) \to w_i^D$

Flexural$_1$ (F_1): $w_1^{AA}(x_1,x_2); w_2^{SS}(x_1,x_2); w_3^{SA}(x_1,x_2) \to w_i^{F_1}$

Flexural$_2$ (F_2): $w_1^{SS}(x_1,x_2); w_2^{AA}(x_1,x_2); w_3^{AS}(x_1,x_2) \to w_i^{F_2}$

Shear (Sh): $w_1^{SA}(x_1,x_2); w_2^{AS}(x_1,x_2); w_3^{AA}(x_1,x_2) \to w_i^{Sh}$.

Here, AS, SA, SS, and AA refer to the parity of a function with respect to the inversion of the variables: $f(x_1,x_2) = f(-x_1,x_2) = f(x_1,-x_2) \to f^{SS}(x_1,x_2)$, $f(x_1,x_2) = -f(-x_1,x_2) = -f(x_1,-x_2) \to f^{AA}(x_1,x_2)$, etc.

For phonon thermal conductivity calculations in nanowires and 1D-QDSLs, we use the following expression, which was derived from the Boltzmann transport equation within the relaxation time approximation[13,27,39] taking into account the one-dimensional density of phonon states:[28]

$$\kappa_{\rm ph} = \frac{1}{2\pi k_B T^2 d_1 d_2} \sum_{\alpha,s} \int_0^{q_{\max}} \left(\hbar\omega_s^\alpha(q)\, v_s^\alpha(\omega(q))\right)^2 \tau_{s,\rm tot}^\alpha(\omega(q)) \times \frac{\exp\left(\frac{\hbar\omega_s^\alpha(q)}{k_B T}\right)}{\left(\exp\left(\frac{\hbar\omega_s^\alpha(q)}{k_B T}\right)-1\right)^2} dq. \tag{9}$$

Here, $\tau_{s,\rm tot}^\alpha(\omega)$ is the total phonon relaxation time, $\alpha = (D, F_1, F_2,$ or Sh) is the polarization index, s is the number of a phonon branch, k_B is the Boltzmann constant, $\hbar$ is the Plank constant, and T is the absolute temperature. In our calculations, we take into account all basic mechanisms of phonon scattering: three-phonon Umklapp, boundary, and impurity scattering.[5–7,28] The total phonon relaxation time is given by $1/\tau_{{\rm tot},s}(q) = 1/\tau_{U,s}(q) + 1/\tau_{{\rm imp},s}(q) + 1/\tau_{B,s}(q)$. Here, (1) $\tau_{U,s}$ is the relaxation time for the Umklapp scattering $\frac{1}{\tau_{U,s}} = \gamma^2 \frac{k_B T\cdot(\omega_s^\alpha)^2}{(\tilde{c}_{44})_s^\alpha V_0\, \omega_{s\max}^\alpha}$,[5,6] where γ is the Grüneisen parameter, V_0 is the volume of an elementary cell, and $(\omega_s^\alpha)_{\max}$ is the maximum phonon frequency of the phonon branch s with the polarization α, $(\tilde{c}_{44}(q))_s^\alpha = \int_{-d_1/2}^{d_1/2}\int_{-d_2/2}^{d_2/2} c_{44}(x_1,x_2)|\vec{w}_s^\alpha(x_1,x_2;q)|^2 dx_1 dx_2$ for a nanowire, and $(\tilde{c}_{44}(q))_s^\alpha = \int_0^L \int_{-d_1/2}^{d_1/2}\int_{-d_2/2}^{d_2/2} c_{44}(x_1,x_2,x_3)|\vec{w}_s^\alpha(x_1,x_2,x_3;q)|^2 dx_1 dx_2 dx_3$ for 1D-QDSLs; (2) $\tau_{\rm imp}$ is the relaxation time for the impurity scattering $\frac{1}{\tau_{{\rm imp},s}} = A\omega_s^4$,[7] where A is a parameter that depends on the concentration of impurities; and (3) $\tau_{B,s}$ is the relaxation time for the boundary scattering, which is an extension of the standard formula for rough edge scattering[38,39] to a rectangular nanowire $\frac{1}{\tau_{B,s}} = \frac{1-p}{1+p}\left(\frac{1}{d_1}+\frac{1}{d_2}\right)\frac{|v_s^\alpha(q)|}{2}$, where $v_s^\alpha(q)$ is the phonon group velocity and p is the specular parameter. In the calculations, we use the following parameters, which are typical for silicon: $\gamma = 0.56$[5] and $A = 1.32\times10^{-9}$ s^3.[7]

III. RESULTS AND DISCUSSION

Due to the elastic stresses in 1D-QDSL structures consisting of materials with small differences in lattice constants (i.e., Si and Ge), the lattice constants along the X and Y axes in the whole 1D-QDSL structures become identical. We assume that the lattice constant of Si/Ge 1D-QDSL structures is equal to a(Si) = 0.543 nm. We have checked that using a(Ge) instead of a(Si) in our calculations or taking into account the dependence of the lattice constant on the coordinate z change the values of thermal conductivity only by a few percent. This implies that taking into consideration the lattice relaxation near Si/Ge interfaces would also weakly change thermal conductivity. To calculate the energy spectra of acoustic phonons in rectangular nanowires, we numerically solve the set represented by Eq. (7) with free boundary conditions in the X_1X_2-plane; i.e., we assume that all force constants outside of the nanostructure are equal to 0. In a 1D-QDSL structure, the number of nonequivalent nodes is equal to the number of nodes on a superlattice period. Therefore, the number of equations in the set represented by Eq. (7) is substantially larger than in a nanowire. For 1D-QDSL, the set in the form of Eq. (7) is solved

by taking into account the periodic boundary conditions along the X_3 axis: $u_i(x_1,x_2,x_3 \pm L,q) = u_i(x_1,x_2,x_3,q)\exp[\pm iqL]$. The calculations are performed for all q values in the interval $(0,\pi/a)$ for nanowires and $(0,\pi/L)$ for 1D-QDSLs. Dispersion relations are obtained for all four phonon polarizations: D, F_1, F_2, and Sh. The energy spectra of dilatational phonons in a homogeneous Si nanowire with a lateral cross section of 4.88 × 4.88 nm and Si/Ge 1D-QDSL structure with the same cross section and eight atomic layers in the superlattice period (six silicon atomic layers and two germanium atomic layers) are shown in Fig. 2. In our calculations, 361 nodes are taken for the Si nanowire and 1444 nodes for Si/Ge 1D-QDSL structure. The total number of phonon branches of dilatational polarization is equal to 280 for a Si nanowire and 1120 for a Si/Ge 1D-QDSL. In Fig. 2, we represent the five lowest phonon branches $\hbar\omega_s(q)$ (with quantum numbers $s = 0, \ldots, 4$) and several higher branches (with $s = 10, 20, 30, \ldots, 200, 300, \ldots, 1100, 1120$). The dashed line in Fig. 2(b) shows the maximal phonon energy in a homogeneous Ge nanowire. The maximal acoustic phonon frequency in silicon is higher than the maximal frequency in germanium; therefore, high-frequency Si-like phonon modes in a Si/Ge 1D-QDSL are "trapped" in the Si segments and do not spread out in the Ge segments of the superlattice. These modes will not participate in the processes of heat transfer; i.e., the 1D-QDSL structure acts as a *phonon filter,* removing many phonon modes from thermal transport. Fig. 2 implies that the velocities of phonon modes with $\hbar\omega > 7$ meV in the Si nanowire are not equal to zero, whereas in a Si/Ge 1D-QDSL, these modes are dispersionless.

An important quantity that determines the value of the phonon thermal conductivity is the average group velocity of phonons[8,17]

$$\langle v\rangle(\omega) = \frac{g(\omega)}{\sum\limits_{s(\omega),\alpha} (v_s(\omega))^{-1}}. \tag{10}$$

Summation in Eq. (10) is performed over all phonon branches s with frequency ω and polarization α; here, $g(\omega)$ is the number of these branches and $v_s = d\omega_s/dq$ is the phonon group velocity for the branch s.

In Fig. 3, we show the dependence of the average phonon group velocity (averaged over all polarizations and branches) on the phonon energy for homogeneous Si and Ge nanowires ($d_1 = d_2 = 4.88$ nm) (solid lines) and the Si/Ge 1D-QDSL ($d_1 = d_2 = 4.88$ nm, $L = 1.9$ nm), with six atomic layers of Si and two atomic layers of Ge per period (dotted line). The average phonon group velocity in the Si/Ge 1D-QDSL is smaller than that in the Ge nanowire for all energies except for the interval $\hbar\omega < 4$ meV, and it is smaller than that in the Si nanowire for all energies. For energies $\hbar\omega > 6$ meV, the average velocity in the Si/Ge 1D-QDSL is 4–6 times lower than that in the Si nanowire. This significant reduction of the average phonon group velocity in a 1D-QDSL is explained by the folding of the phonon modes with high frequencies in the Si segments of superlattice, and as demonstrated later, it strongly decreases lattice thermal conductivity in a 1D-QDSL in comparison with a nanowire.

For numerical calculations of lattice thermal conductivity in nanowires and 1D-QDSL structures, we performed numerical integration in Eq. (9) using phonon dispersions $\hbar\omega_s(q)$ and total phonon scattering rates $1/\tau_{\mathrm{tot},s}(q)$ calculated for each phonon branch s.

The specular parameter p of boundary scattering is an important parameter that influences the value of thermal conductivity in nanostructures.[6,28,38] The thermal conductivities of thin films or nanowires in purely specular boundary scattering ($p = 1$) are several times larger than those in purely diffusive scattering ($p = 0$). However, our calculations show that the ratio of thermal conductivity values in the analyzed 1D-QDSLs and in nanowires varies by 10%–15% with changing p. Therefore, for all nanostructures considered in the present work, we used $p = 0.85$, which was found in Ref. 28 from comparison between theoretical and experimental data for thin Si film with thickness of 20 nm.

In Fig. 4, lattice thermal conductivity is plotted as a function of temperature for the Si and Ge nanowires with a cross section of 4.88 × 4.88 nm and for the Si/Ge 1D-QDSL with the same cross section and eight atomic layers in a period ($L = 1.9$ nm). The presented graph implies that the lattice thermal conductivity of the considered Si/Ge 1D-QDSL is significantly lower than that in the corresponding generic Si or Ge nanowires. In the temperature range 150–300 K, thermal conductivity in the 1D-QDSL is 5–6 times lower than that in the Ge nanowire with the same cross section and 9–11 times lower than that in the Si nanowire. When the number of atomic layers of Si per period increases from four to six (Fig. 4), the properties of the Si/Ge 1D-QDSL reveal a slight trend toward those of the Si nanowire. Therefore, the phonon

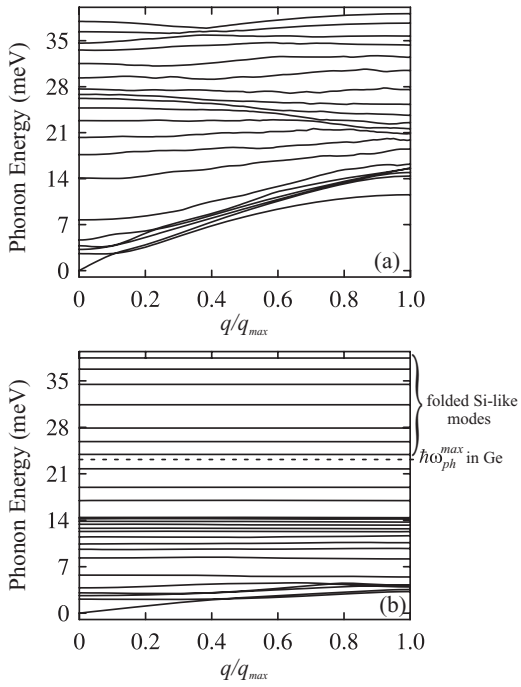

FIG. 2. Dilatational phonon energies as a function of the phonon wave vector q in (a) a homogeneous rectangular Si nanowire and (b) a Si/Ge 1D-QDSL. In (a), the lateral cross section is 4.88 × 4.88 nm, and the phonon branches with $s = 0$ to 4, 10, 30, 50, ..., 280 are shown. In (b), the lateral cross section is the same, and there are eight atomic layers per superlattice period (two atomic layers of Ge and six atomic layers of Si). The phonon branches with $s = 0$ to 4, 10, 30, 50, ..., 190, 200, 300, ..., 1100, 1120 are depicted.

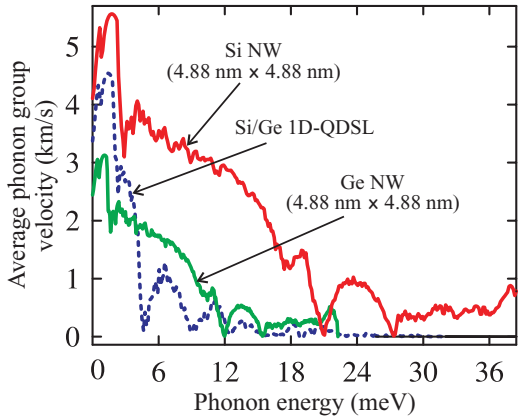

FIG. 3. (Color online) Average phonon group velocity as a function of the phonon energy in Si and Ge homogeneous nanowires with the lateral cross section 4.88 × 4.88 nm and in Si/Ge 1D-QDSL with the same lateral cross section and eight atomic layers per superlattice period (two atomic layers of Ge and six atomic layers of Si).

thermal conductivity in the Si/Ge 1D-QDSL, containing an equal number of atomic layers of Si and Ge, is lower than in the 1D-QDSL, containing different numbers of atomic layers per period (Fig. 4).

In Ref. 24, it is theoretically shown that thermal conductivity of 1D-QDSLs (segmented nanowires), consisting of different isotopes of silicon, is by a factor of two smaller than in a Si nanowire. Our results demonstrate an even greater drop in thermal conductivity in 1D-QDSL composed of segments from acoustically mismatched materials due to a stronger localization of phonon modes in the superlattice segments and a stronger decrease in phonon group velocities. Our findings for the Si/Ge 1D-QDSL are in line with the reduction of thermal conductivity down to the sub-1 W m^{-1} K^{-1} range achieved recently in multilayered Ge/Si dot arrays.[19] A similar effect of a strong decrease of thermal conductivity is demonstrated theoretically in Ref. 40 for three-dimensional

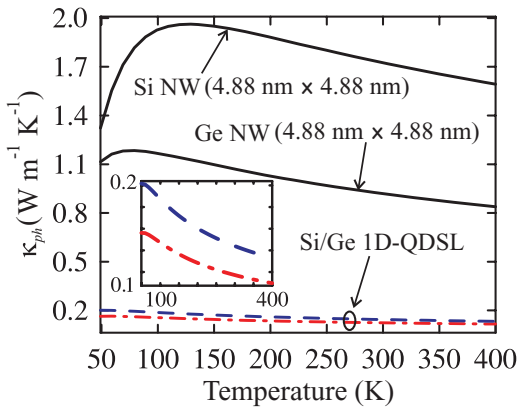

FIG. 4. (Color online) Temperature dependence of lattice thermal conductivity for Si and Ge homogeneous nanowires (solid lines) and for Si/Ge 1D-QDSLs, with six atomic layers of Si and two atomic layers of Ge (dashed line) and with four atomic layers of Si and four atomic layers of Ge (dash-dotted line) per superlattice period. The inset shows a magnified view of the above temperature dependence of thermal conductivity for 1D-QDSLs.

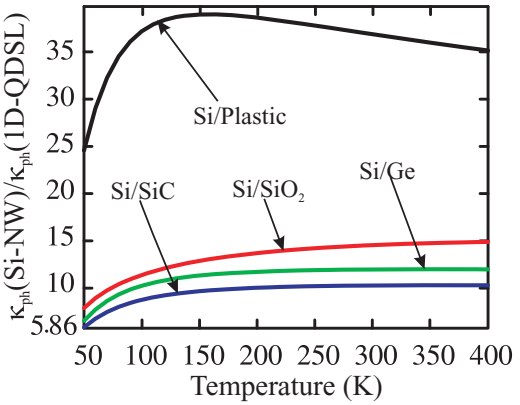

FIG. 5. (Color online) Temperature dependence of the ratio between lattice thermal conductivity in an Si nanowire and that in different 1D-QDSLs with six atomic layers of Si and two atomic layers of an acoustically-mismatched material (Ge, plastic, SiC, or SiO_2) per superlattice period.

Si/Ge quantum-dot superlattices in the framework of a lattice-dynamics model with Stillinger-Weber potentials. The authors of Ref. 40 explain the thermal conductivity reduction by the significant decrease in phonon group velocities and incoherent scattering of the particle-like phonons.

Figure 5 illustrates the drop in thermal conductivity in a 1D-QDSL consisting of segments made of Si, Ge, and model materials, in comparison with the Si nanowire with the same cross section 4.88 × 4.88 nm. As an example of a material with a higher longitudinal sound velocity than that in silicon, we choose SiC. As examples of materials with lower sound velocities, a plastic and SiO_2 are selected. For the calculation of the phonon energy spectra in 1D-QDSL with model materials, we assumed that these materials possess the same crystal structure as Si with the lattice constant $a = a(\mathrm{Si})$ but have elastic constants of the corresponding material: plastic, SiO_2, or SiC. Generally, more complicated lattice-dynamics models than the FCC model are needed for an accurate quantitative description of 1D-QDSL structures with acoustically mismatched quantum dots. Therefore, in 1D-QDSL structures composed of model materials, our results provide a qualitative description of thermal conductivity. The elastic constants and mass density of plastic, SiO_2, and SiC taken for our calculation are presented in Table I. A specific chemical nature of the model plastic material is not essential for our analysis. We assume that the sound velocity in plastic material is 2000 m s^{-1} and the mass density is 1 g cm^{-3}. The chosen values of these parameters correspond to those of a large number of

TABLE I. Materials parameters of plastic, SiO_2, and SiC.

	c_{11} (GPa)	c_{12} (GPa)	c_{44} (GPa)	ρ (g cm^{-3})
Plastic[a]	4.0	2.0	1.0	1.0
SiO_2[b]	76.6	14.8	30.9	2.2
SiC[c]	290.0	235.0	55.0	3.2

[a]References 9 and 41.
[b]Calculated from longitudinal and transverse sound velocities, which are taken from Ref. 42.
[c]Reference 43.

plastic materials (e.g., polyvinyl chloride, polystyrene, or polyethylene).[41]

In the Si/plastic 1D-QDSL, the average phonon group velocity strongly decreases due to the decelerating effect of the plastic material and dispersionless phonon modes folded in the superlattice segments. An interplay between these two effects leads to a decrease of thermal conductivity by a factor of 25–35 in comparison with that of the Si nanowire. Thermal conductivity of the Si/SiC and Si/SiO_2 1D-QDSL is lower than that in the Si nanowire by factors of 5–10 and 8–15, respectively, depending on the temperature. A similar dramatic influence of the acoustically mismatched layers on the phonon properties and thermal conductivity is theoretically reported in Refs. 3,11, 22,23, and 28 for planar heterostructures and coated nanowires. The predicted effect of the phonon filtering can be achieved in the strain-induced self-organized nanoarchitectures, e.g., rolled-up radial superlattices,[44–46] which comprise alternating crystalline and amorphous, as well as inorganic and organic, layers.

IV. CONCLUSIONS

We investigated the phonon and heat-conducting properties of 1D-QDSLs of Si/Ge, Si/plastic, Si/SiC, and Si/SiO_2 consisting of acoustically mismatched materials in the framework of the FCC model of lattice dynamics. Numerous phonon branches with low group velocities appear in 1D-QDSL structures in comparison with a generic nanowire. A drop in the group velocities in 1D-QDSL structures leads to a strong decrease of their lattice thermal conductivity compared with that of a homogeneous nanowire. 1D-QDSL structures act as effective phonon filters, eliminating a part of high-energy phonon modes from the heat flux. As a result, the considered 1D-QDSLs demonstrate ultralow sub-1 W m^{-1} K^{-1} thermal conductivity in the wide temperature range of 50–400 K. The obtained results indicate that 1D-QDSL structures are good candidates for thermoelectric and thermoisolation applications.

ACKNOWLEDGMENTS

The work was supported by the International Bureau of the Bundesministerium für Bildung und Forschung under Project No. MDA 09/007 and the Deutsche Forschungsgemeinschaft SPP 1386 under Project No. RA1634/5-1 (Germany), as well as by the Moldova State under Projects No. 10.820.05.02GA, 11.817.05.10F and 10.819.05.02F. The work at University of California–Riverside was supported in part by the Semiconductor Research Corporation and Defense Advanced Research Projects Agency (DARPA) through the Focus Center Research Program's Center on Functional Engineered Nano Architectonics and DARPA's Defense Microelectronics Activity under Agreement No. H94003-10-2-1003.

*dlnika@yahoo.com

[1] D. G. Kahill, W. K. Ford, K. E. Goodson, G. D. Mahan, A. Majumdar, H. J. Maris, R. Merlin, and S. P. Phillport, J. Appl. Phys. **93**, 793 (2003).
[2] A. Shakouri, Proc. IEEE **94**, 1613 (2006).
[3] A. A. Balandin, E. P. Pokatilov, and D. L. Nika, J. Nanoelectron. Optoelectron. **2**, 140 (2007).
[4] A. Khitun, A. Balandin, J. L. Liu, and K. L. Wang, J. Appl. Phys. **88**, 696 (2000).
[5] A. Balandin and K. L. Wang, Phys. Rev. B **58**, 1544 (1998).
[6] J. Zou and A. Balandin, J. App. Phys. **89**, 2932 (2001).
[7] N. Mingo, Phys. Rev. B **68**, 113308 (2003).
[8] E. P. Pokatilov, D. L. Nika, and A. A. Balandin, Superlatt. Microstruct. **38**, 168 (2005).
[9] E. P. Pokatilov, D. L. Nika, and A. A. Balandin, Superlatt. Microstruct. **33**, 155 (2003).
[10] D. Li, Y. Wu, P. Kim, L. Shi, P. Yang, and A. Majumdar, Appl. Phys. Lett. **83**, 3186 (2003).
[11] X. Lu and J. Chu, J. Appl. Phys. **101**, 114323 (2007).
[12] J. Zou, D. Kochetkov, A. A. Balandin, D. I. Florescu, and F. H. Pollak, J. Appl. Phys. **92**, 2534 (2002).
[13] S. G. Volz and G. Chen, Appl. Phys. Lett. **75**, 2056 (1999).
[14] X. Lu, J. H. Chu, and W. Z. Shen, J. Appl. Phys. **93**, 1 (2003).
[15] A. Khitun, A. Balandin, and K. L. Wang, Superlatt. Microstruc. **26**, (1999).
[16] I. Ponomareva, D. Srivastava, and M. Menon, Nano Lett. **7**, 1155 (2007).
[17] E. P. Pokatilov, D. L. Nika, and A. A. Balandin, Phys. Rev. B **72**, 113311 (2005).
[18] S. I. Tamura,Y. Tanaka, and H. J. Maris, Phys. Rev. B **60**, 2627 (1999).
[19] G. Pernot, M. Stoffel, I. Savic, F. Pezzoli, P. Chen, G. Savelli, A. Jacquot, J. Schumann, U. Denker, I. Monch, C. Deneke, O. G. Schmidt, J. M. Rampnoux, S. Wang, M. Plissonnier, A. Rastelli, S. Dilhaire, and N. Mingo, Nat. Mater. **9**, 491 (2010).
[20] J. L. Liu, A. Khitun, K. L. Wang, W. L. Liu, G. Chen, Q. H. Xie, and S. G. Thomas, Phys. Rev. B **67**, 165333 (2003).
[21] O. L. Lazarenkova and A. A. Balandin, Phys. Rev. B **66**, 245319 (2002).
[22] J. Zou, X. Lange, and C. Richardson, J. Appl. Phys. **100**, 104309 (2006).
[23] D. L. Nika, N. D. Zincenco, and E. P. Pokatilov, J. Nanoelect. Optoelect. **4**, 170 (2009).
[24] N. Yang, G. Zhang, and B. Li, Nano Lett. **8**, 276 (2008).
[25] A. Ward and D. A. Broido, Phys. Rev. B **81**, 085205 (2010).
[26] N. Mingo, L. Yang, D. Li, and A. Majumdar, Nano Lett. **3**, 1713 (2003).
[27] N. Mingo, Phys. Rev. B **68**, 113308 (2003).
[28] D. L. Nika, N. D. Zincenco, and E. P. Pokatilov, J. Nanoelect. Optoelect. **4**, 180 (2009).
[29] M. S. Gudiksen, L. J. Lauhon, J. Wang, D. C. Smith, and C. M. Lieber, Nature **415**, 617 (2002).
[30] M. T. Bjork, B. J. Ohlsson, C. Thelander, A. I. Persson, K. Deppert, L. R. Wallenberg, and L. Samuelson, Appl. Phys. Lett. **81**, 4458 (2002).
[31] M. T. Bjork, B. J. Ohlsson, T. Sass, A. I. Persson, C. Thelander, M. H. Magnusson, K. Deppert, L. R. Wallenberg, and L. Samuelson, Nano Lett. **2**, 87 (2002).

[32]Y.-C. Wen, J.-H. Sun, C. Dais, D. Grützmacher, T.-T. Wu, J.-W. Shi, and C.-K. Sun, Appl. Phys. Lett. **96**, 123113 (2010).
[33]Y. M. Lin and M. S. Dresselhaus, Phys. Rev. B **68**, 075304 (2003).
[34]V. M. Fomin and P. Kratzer, Phys. Rev. B **82**, 045318 (2010).
[35]P. N. Keating, Phys. Rev. B **145**, 637 (1966).
[36]M. Born and K. Huang, *Dynamic Theory of Crystal Lattices* (Oxford University Press, Oxford, 1954).
[37]G. Leibfried and W. Ludwig, in *Solid State Physics*, Vol. 12, edited by F. Seitz and D. Turnbull (Academic, New York, 1961), pp. 275–444.
[38]J. M. Ziman, *Electrons and Phonons* (Clarendon Press, Oxford, 2001), p. 463.
[39]D. L. Nika, E. P. Pokatilov, A. S. Askerov, and A. A. Balandin, Phys. Rev. B **79**, 155413 (2009).
[40]J.-N. Gillet, Y. Chalopin, and S. Volz, J. Heat Trans. **131**, 043206 (2009).
[41]See, for example [http://www.bamr.co.za/velocity%20of%20materials.shtml].
[42]V. A. Fonoberov and A. A. Balandin, Nano Lett. **6**, 2442 (2006).
[43]See, for example [http://www.ioffe.ru/SVA/NSM/Semicond/SiC/mechanic.html].
[44]Ch. Deneke, N.-Y. Jin-Phillipp, I. Loa, and O. G. Schmidt, Appl. Phys. Lett. **84**, 4475 (2004).
[45]Ch. Deneke, U. Zschieschang, H. Klauk, and O. G. Schmidt, Appl. Phys. Lett. **89**, 263110 (2006).
[46]Ch. Deneke, R. Songmuang, N.-Y. Jin-Phillipp, and O. G. Schmidt, J. Phys. D Appl. Phys. **42**, 103001 (2009).